RSC Advances

PAPER

View Article Online
View Journal | View Issue

Check for updates

Cite this: *RSC Adv.*, 2024, **14**, 8378

# A new magneto-optical phenomenon enhanced by Au nanoparticles on 3D Ni sub-microstructures†

Chenxin Zhou, * Qingtong Wang, Changlin Dong, Jiajun Gu * and Di Zhang

Received 20th July 2023
Accepted 1st March 2024

DOI: 10.1039/d3ra04898e

rsc.li/rsc-advances

We constructed a bio-structured surface-plasmonic/magneto-optic composite of ferromagnet metal Ni and noble metal Au. It was found that Ni *Morpho menelaus* (Mm) butterfly wings (BWs) with a natural photonic crystal structure have an apparent enhancement of light reflection under a 0.3 T magnetic field. Additional introduction of discrete Au particles helps further increase this magnetism-induced response. Compared with Mm-Ni-BWs, Mm-Ni–Au30-BWs' reflectance increases 5.3 times at 1944 nm. This investigation helps reveal and understand the effects of new micro-nanostructures on surface plasmon/magneto-optic coupling, benefiting future applications of biology sensors, chemical sensors, photonic chips, electrical communication systems, *etc.*

Open Access Article. Published on 11 March 2024. Downloaded on 7/24/2025 9:55:34 AM.
This article is licensed under a Creative Commons Attribution-NonCommercial 3.0 Unported Licence.

## 1. Introduction

The discovery of surface plasmon sparked interest in surface-enhanced polarized waves influenced by external magnetic fields, giving birth to the concept of magneto plasmon (MP).[1–3] With the progress of nanomachine tools and nanotechnology, new nanostructures are emerging constantly, and magneto-optical (MO) recording of plasmon resonance and magnetic field interaction has made great progress.[4–7] In addition to having a second-level conversion speed comparable to external photon regulation, external magnetic field regulation can also change the polarization state of light waves under high intensity conditions.[8] Plasmon resonance can effectively reduce the size of the device while enhancing the magneto-optical response, which is expected to solve the problem of the realization of the basic components (such as modulator converter multi-channel transmitters and couplers, *etc.*) in nano-photonic chips.

There are two key factors that determine the performance of a magnetic surface plasmon system: magneto-optical response and optical wave loss. When a ferromagnet is subjected to a small external magnetic field, the dielectric tensor changes from symmetric to asymmetric. The Kerr effect in the transmission direction and Faraday rotation in the reflection direction both occur obviously, showing a strong magneto-optical response. However, ferromagnets have large optical wave loss, and the plasmon resonance is mostly in the visible light range with a wide wavelength.[8] In comparison, precious metals can effectively reduce light wave loss and achieve plasmon resonance at precise wavelengths,[9] but the magneto-optical response of precious metals is much weaker under the same external conditions. Therefore, it is promising to combine the high magneto-optical response of the ferromagnet and the plasmon resonance effect of the precious metal, to enhance the magneto-optical effect generated by the surface plasmon excitation.[10–13]

To develop nanostructures for magnetic surface plasmon applications, several problems are yet to be solved. First, the manufacturing process is complex and expensive. Second, the electromagnetic field inside the nanostructure presents nonlinear distribution. Currently, the nanostructure prepared by artificial physical and chemical methods is relatively limited, which is not easy to be refined and is complicated. It is difficult to perfectly match the magnetic surface plasmon effect, limiting the further development of magnetic surface plasmon system. Third, the mechanism of MP effect has not been studied deeply enough. More nanostructures need to be created as model materials to deepen researchers' understanding of the physical principle and coupling process behind MP effect.

Nature provides solution to solve the above problems. After billions of years of evolution, various natural species have developed a large number of complex and fine structures, which are perfect natural optical materials showing excellent optical properties. Tan *et al.* developed a versatile approach to fabricate intact 3D metallic butterflies with a sub-micrometer level spatial resolution.[14–16] Using periodic structures as templates, new micro-nano structured optical materials can be prepared by manually converting their components into functional materials while retaining the natural fine-graded periodic structures. These materials have fine and complex micro–nano structures. This feature can match the electromagnetic field distribution under the influence of different materials and realize the coupling of material characteristics and natural structures, which is benefit for the study of the simulation process and the

*School of Materials Science and Engineering, Shanghai Jiao Tong University, Shanghai, China. E-mail: zhouchenxin@sjtu.edu.cn; gujiajun@sjtu.edu.cn*

† Electronic supplementary information (ESI) available. See DOI: https://doi.org/10.1039/d3ra04898e



© 2024 The Author(s). Published by the Royal Society of Chemistry

Open Access Article. Published on 11 March 2024. Downloaded on 7/24/2025 9:55:34 AM. This article is licensed under a Creative Commons Attribution-NonCommercial 3.0 Unported Licence.

essential mechanism. In addition, these materials have several advantages including easy to fabricate, low cost, and difficult to prepare *via* other artificial methods, *etc.*

Here we use two types of butterfly wings (BWs), *i.e.*, *Papilio paris* (Pp) and *Morpho menelaus* (Mm), as templates, to successfully fabricate a surface-plasmonic/magneto-optic composite with 3D sub-microstructures (Ni–Au30-BWs). The magneto-optical effect of the material in a wide spectrum of 250–2500 nm is also investigated. The influence of 3D sub-microstructures and Au surface states on the magneto-optical effect are studied. This research will enlarge the practical application of magneto-optical effect. It can be used to make wide spectrum response of magneto-optical switch or optical isolators, which is an important way to achieve optical non-reciprocity and plays an important role in optical communication and lasers.

## 2. Experimental

### 2.1 Materials

Chloroauric acid ($HAuCl_4 \cdot 4H_2O$, Au ≥ 47.8%), ethyl alcohol (EtOH, 99.7%), ethyldiamine (EDA), sodium hydroxide (NaOH, 98%), tartaric acid (TA, 99%), citric acid (CA, 99%), trisodium citrate dihydrate ($Na_3C_6H_5O_7 \cdot 2H_2O$, 99%), nickel sulfate ($NiSO_4 \cdot 6H_2O$, ≥98.5%), dimethylamine borane (DMBA, 95.0%), sodium borohydride ($NaBH_4$, 98.0%), ammonium hydroxide ($NH_3 \cdot H_2O$), lactic acid (≥85%) were purchased from Sinopharm Chemical Reagent. Cysteamine (Cysa, 98%) was purchased from Energy Chemical Co. Ltd. *Papilio paris* (Pp) and *Morpho menelaus* (Mm) were purchased from Shanghai Qiuyu Co. Ltd. All chemicals were used as received without further purification.

### 2.2 Fabrication of Ni butterfly wings

First, BWs were washed in redistilled water for three times and then dipped in EtOH for 20 min. The BWs were successively immersed in 1 M NaOH solution and ethyldiamine ethanol solution (25%) for 2–4 hours for hydrophilization. Then the BWs were soaked in a chloroauric acid solution (0.5%) for 4 hours to bond gold ions. After being rinsed completely, 40 mL of $NaBH_4$ solution (2%) was used to reduce the bonded gold ions to metallic clusters. Note that the BWs must be washed by redistilled water for three times between each step. Then Au seeded BWs were put into a growth solution (100 mL) that consists of 98 mL of redistilled water, 2 g of $NiSO_4 \cdot 6H_2O$, 1 g of $NaBH_4$, 0.5 mL of lactic acid, 1.5 mL of $NH_3 \cdot H_2O$, and 0.1 g of DMBA. During the growth, we shook the reactor to remove the produced hydrogen gas. After 5 to 10 min, Ni-butterfly-wings was obtained and rinsed in redistilled water for three times to get rid of the adsorbed growth solution.

### 2.3 Synthesis of citrate-Au nanospheres (Au NSP 30)

Citrate-stabilized nanospheres were prepared by adding 5 mL (for Au NSP 30) of 1% citrate solution to 100 mL of boiling 1 mM $HAuCl_4$ solution (2.06 mL of 48.6 mM) under vigorous stirring. After boiling for 15 min, the solution was cooled down to room temperature. The solution volume was kept constant during

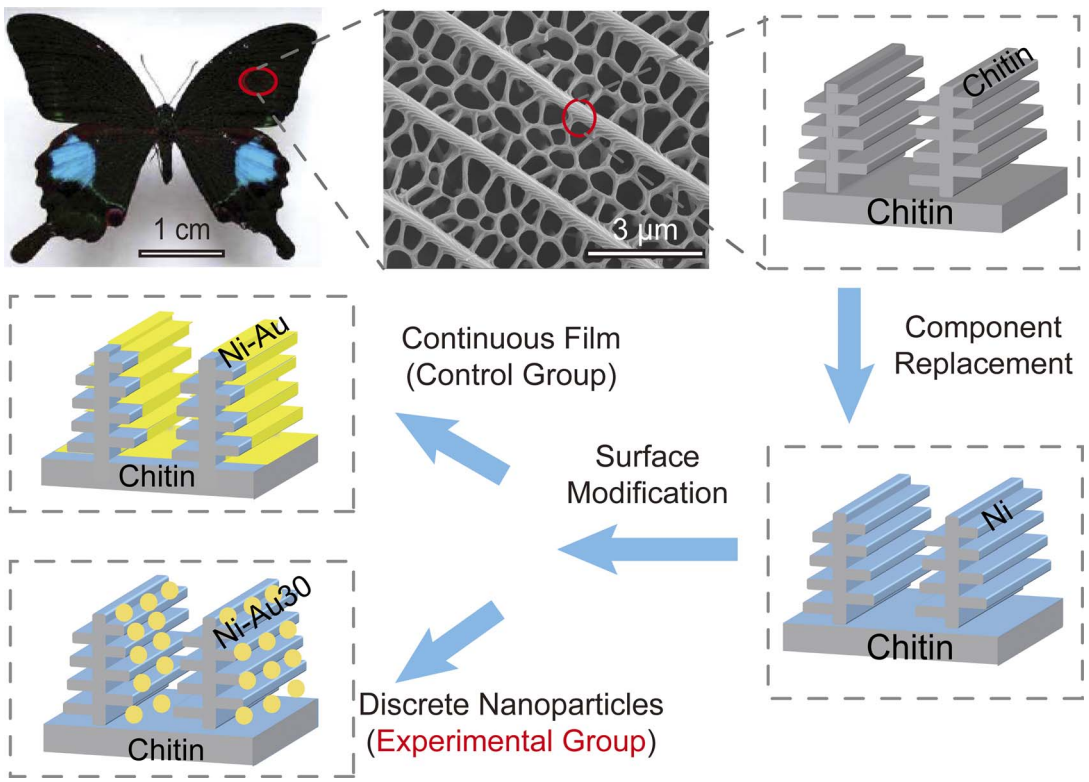


Fig. 1 Schematic of replicating Pp wings into 3D bi-metal structures.

Open Access Article. Published on 11 March 2024. Downloaded on 7/24/2025 9:55:34 AM. This article is licensed under a Creative Commons Attribution-NonCommercial 3.0 Unported Licence.

boiling. The nanoparticle solutions for assembly or for nanostar growth were stored at 4 °C. The particle size distribution was determined by randomly measuring 200 particles from TEM images.

### 2.4 Templates for assembly

Amination of Ni BWs for assembly. Before assembly, Ni butterfly wings were incubated in a 10 mM cysa solution at 25 °C for 6 h, followed by washing with plenty of water to remove the dissociative cysa and drying in air. The aminated Ni-BWs were soaked in 200 mL of nanoparticle solutions with pH values adjusted from 4.8 to 5.2 by adding NaOH or citric acid. After 24–72 hours assembly, Ni–Au30 BWs was washed using redistilled water and dried in air.

## 3. Result and discussion

The BWs are composed of overlapping microscales, which form two or more layers over the wing membrane. The Pp is quasi-honeycomb-structured (Fig. 1), and Mm is dendritic-structured. Because of their different 3D sub-microstructures, BWs have different structural colours, especially for the Mm as a natural photonic crystal.[17] Therefore, using the BWs as a template, Ni–Au composites with 3D sub-microstructures have great significance for the research of magneto-optical phenomena. First, we pretreated the BWs to improve their surface hydrophilicity. Then the chemical plating method was used to fabricate Ni BWs, where the continuous Ni film was attached to the chitin surface by complexation.[15] At last, we modified the surface of Ni BWs with two different states of Au: chemically plated continuous Au films and self-assembled Au nanoparticles. We measured the size of Au nanoparticles to be 30 nm in ESI (Fig. S1†). After chemical coating and self-assembling, the original BWs' hierarchical structure is successfully retained (Fig. 2a and e).

Scanning electron microscopy (SEM) and transmission electron microscopy (TEM) images provide further insight into the morphologies and microstructures of these two kinds of butterflies, *i.e.*, Pp Ni-BWs (Fig. 2a) and Mm Ni–Au30 BWs (Fig. 2e). The seamless, continuous shell at the contacting junction between the ridges and the scale bottom suggests that the Pp Ni–Au30 BWs (Fig. 2b) and Mm Ni–Au30 BWs (Fig. 2f) retained the overall scale morphology of the original BW. In the mapping results (Fig. 2c and g), it can be found that the continuous Ni film was plated on the surface of BWs structure, while the Au nanoparticles were distributed discretely on Ni. The Ni crystal lattice parameter of (111) plane is 0.25 nm, which is same (0.25 nm) as reported in literature,[18] marked as the red lines in Fig. 2d and h. The Au crystal lattice parameter of (111) plane is 0.232 nm, which is nearly same (0.23 nm) as reported in literature,[19] marked as the green lines in Fig. 2d and h.

X-ray diffraction (XRD) was used to determine the structure of Ni BWs (Fig. S4†) and Ni–Au30 BWs (Fig. 3a). As compared to the XRD standard PDF card, Au (111), (200), (311), (222) (PDF: 99-0056) and Ni (111) (PDF: 87-0712) scores were obtained. This result is consistent with crystal lattice images from Fig. 2d and h. The reflectance spectra were measured *via* a spectrophotometer (PerkinElmer Lambda 750s). To analyse the magneto-optic effects, we measured the reflectance (250–2500 nm) spectra of Ni-BWs (Fig. 3b) and Ni–Au30 BWs (Fig. 3c) under a 0.3 T magnetic field, which is perpendicular to the BWs (Fig. 3f). The reflectance of two Ni BWs was changed less than 4% (inset Fig. 3b) at the reflection peak at 1944 nm. Compared to the Ni-BW samples without the help from Au particles, the reflectance spectrum of Ni–Au30 BWs increased from 3.8% to 12.7% and 3.7% to 19.6% for Pp and Mm, respectively (Fig. 3d). It can be concluded that discrete Au nanoparticles amplify the magneto-optical effect due to its localized surface plasmon resonance (LSPR). The Mm with the natural photonic crystal configuration had a 5.3-times variation. When the size of Au nanoparticles is 30 nm, it had exhibited a characteristic LSPR maximum at 525 nm.[20] The reflectance changes under the 0.3 T magnetic field for these two Ni BWs were both less than 4% (inset of

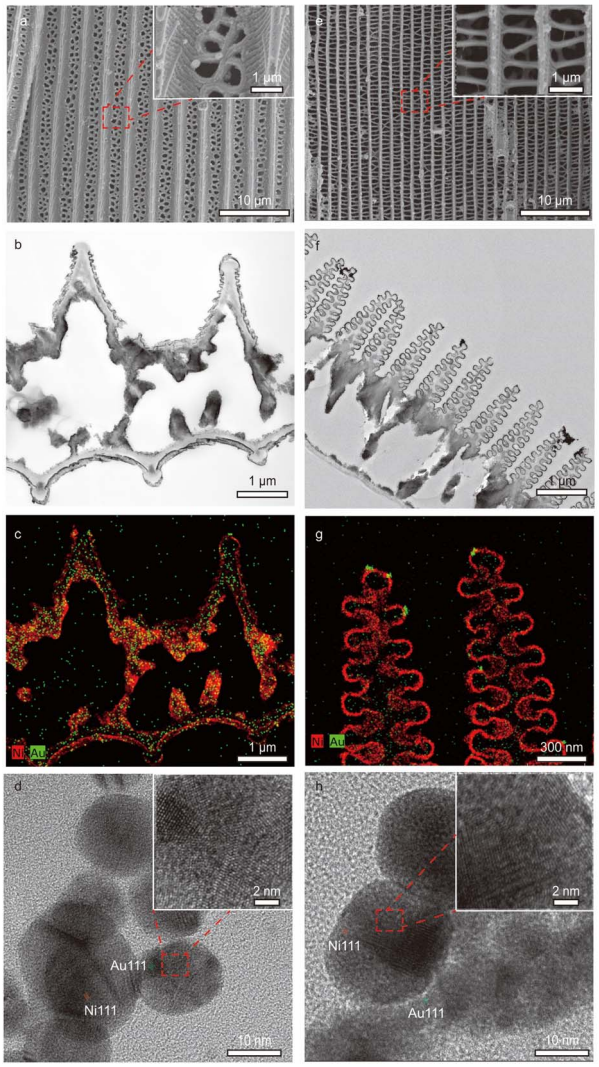


Fig. 2 Structural characterizations for (a–d) Pp Ni–Au30 BWs and (e–h) Mm Ni–Au30 BWs. First row: SEM images; second row: TEM images of the samples' cross-section; third row: elemental mapping results of the second row; fourth row: HRTEM characterizations.


© 2024 The Author(s). Published by the Royal Society of Chemistry

Open Access Article. Published on 11 March 2024. Downloaded on 7/24/2025 9:55:34 AM.
This article is licensed under a Creative Commons Attribution-NonCommercial 3.0 Unported Licence.

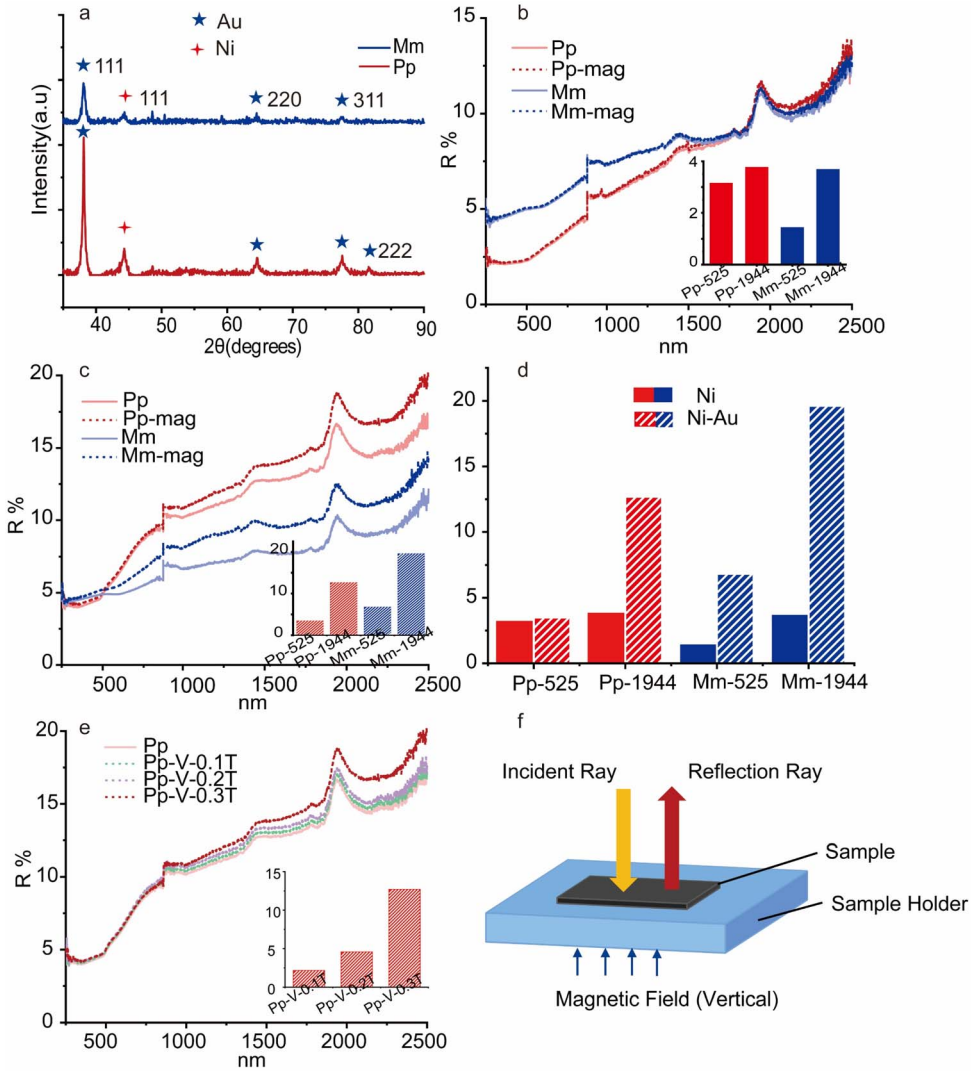


Fig. 3 (a) XRD results of Ni–Au30 BWs; (b) reflectance spectra of Ni BWs; (c) reflectance spectra of Ni–Au30 BWs; (d) comparison of magneto-optical effect differences for various samples; (e) Pp-Ni–Au30 BWs' reflectance spectra under different magnetic fields; (f) schematic of the experimental set-up for reflectance measurements under various applied magnetic fields.

Table 1 Summary of magnetic properties of Pp-Ni–Au30 BWs

| Materials | Coercivity (Oe) | Remanence (emu $g^{-1}$) | Approximate saturation (Oe) | Saturation magnetization (emu $g^{-1}$) |
|---|---|---|---|---|
| Pp-Ni-10 min–Au30 | 80 | 1.43 | 6000 | 7.74 |
| Pp-Ni-10 min | 60 | 1.91 | 6000 | 11.69 |

Fig. 3b) at 525 nm. Compared with Ni-BWs, the Ni–Au30 BWs reflectance spectrum of Mm increased from 1.4% to 6.8% (Fig. 3d), while Pp have no noticeable change. Comparing Fig. 2b–f, we can find that the ridges of both Pp and Mm are tree-like.[15] Those sub-ridge structures, or "branches", benefit coupling lights into plasmonic metals.[16] This is the reason why both Pp and Mm show reflectivity changes. However, the Pp structure has 5–7 layers, less than the 10–12 layers of Mm structure, making its optical response weaker than Mm.[16] The pretreatments of BWs were mainly for hydrophilization rather than decolorization. Hence, there were some remaining pigments in the sample, causing Pp and Mm were slightly different in color and also affecting the baselines of spectra in Fig. 3c.

The reflectance spectrum of Pp-Ni–Au30 BWs changes with the intensity of applied magnetic fields (Fig. 3e, V denotes that the magnetic field is vertical to the sample surface). The reflectance of Pp-Ni–Au30 BWs at 1944 nm enhances from 2.2%

Open Access Article. Published on 11 March 2024. Downloaded on 7/24/2025 9:55:34 AM.
This article is licensed under a Creative Commons Attribution-NonCommercial 3.0 Unported Licence.

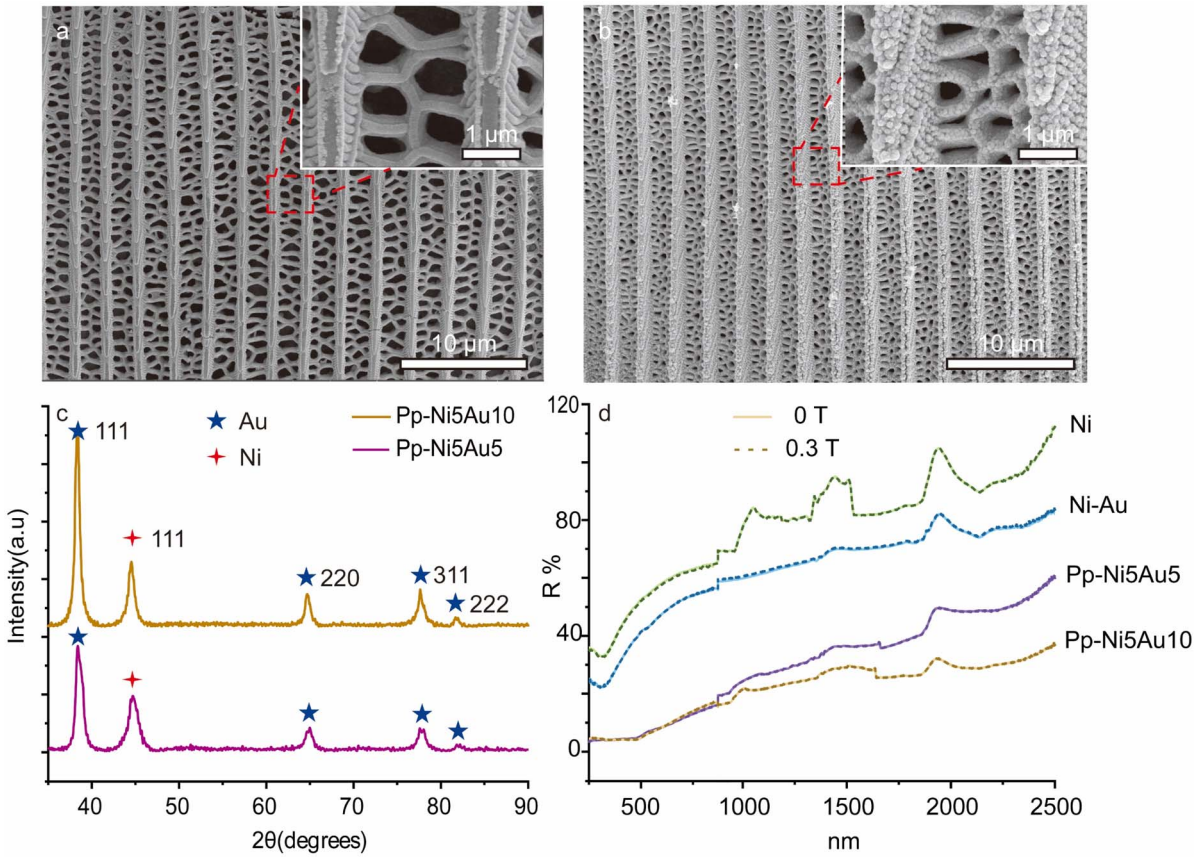


Fig. 4 (a) and (b) SEM images of Pp-Ni5minAu5min and Pp-Ni5minAu10min respectively; (c) XRD results of Pp-Ni5minAu5min and Pp-Ni5minAu10min; (d) Reflectance spectra of the comparison experiment.

(0.1 T) to 4.6% (0.2 T), and achieves 12.7% under 0.3 T, confirming the increase in reflectance with the vertically applied magnetic fields. The intensity of magnetic field was calibrated *via* a KT101 handheld Tesla meter.

Since the reflectance of Pp-Ni–Au30 BWs increases with the vertically applied magnetic fields, we further investigate the magnetic properties of Pp-Ni–Au30 BWs and Pp-Ni BWs. The hysteresis loops were measured using a magnetic performance measurement system (MPMS3). From the hysteresis loops presented in Fig. S2,† several magnetic parameters can be determined (Table 1). Both Pp-Ni-10 min–Au30 and Pp-Ni-10 min have small coercive forces and low saturation magnetizations, which exhibit nearly super-paramagnetic behaviors.[21]

To further analyse the influence of structure and Au nanoparticles on magneto-optical effect, we have designed several control experiments. First, we compared the Ni sheet and Au nanoparticles self-assembled on the surface of Ni sheets. The Ni sheets have smooth surface (Fig. S3†). Second, we compared the Pp-Ni BWs fabricated with two electroless Au plating time (5 and 10 min). Both samples have continuous Au film (Fig. 4a and b). When the applied magnetic field was 0.3 T, the reflectance spectra of Ni sheet, Ni sheet–Au nanoparticles, and Pp BWs (Ni 5 min, Au 5 min; Ni 5 min, Au 10 min) barely changed (Fig. 4d).

Through comparative experimental analysis, this magneto-optical phenomenon appears on three-dimensional structure Ni with discrete Au nanoparticles. Combining with the results in Fig. 3e and S2,† we speculate that this phenomenon might originate from a structural change of the BWs under the applied magnetic field.[22] It was reported that the addition of external magnetic field can lead to a structural shrinkage, which will cause a slight shift for the reflection peak.[22] We thus conducted finite-difference time-domain (FDTD) simulations for Pp-Ni–Au BWs (Fig. 5a) and Pp-Ni BWs (Fig. S5a†). The ridge structure and "window" structure of Pp BWs were reduced to a tree-like unit (P1, Fig. 5c) and a regular honeycomb unit (P2, Fig. 5c), respectively. According to our analyses on SEM characterizations, the height and spacing of P1 were set to be 1.68 μm and 0.27 μm, respectively, and the P2 thickness was set to be 2.15 μm. Results show that when the height and layer spacing of P1 decreased to 1.51 μm and 0.24 μm under magnetic field (~10% structural shrinkage from its original magnetic-field-free counterpart[22]), respectively, the reflection could somewhat increase (Fig. 5d). However, compared with Pp-Ni BWs (red dashed line), the reflection of Pp-Ni–Au30 BWs (blue dashed line) exhibited significant enhancement under magnetic field. This additional increase in reflection might originate from a coupling effect between LSPR of Au nanoparticles and the structural changes under magnetic field. In-depth studies are still underway at present.


© 2024 The Author(s). Published by the Royal Society of Chemistry

Open Access Article. Published on 11 March 2024. Downloaded on 7/24/2025 9:55:34 AM.
This article is licensed under a Creative Commons Attribution-NonCommercial 3.0 Unported Licence.

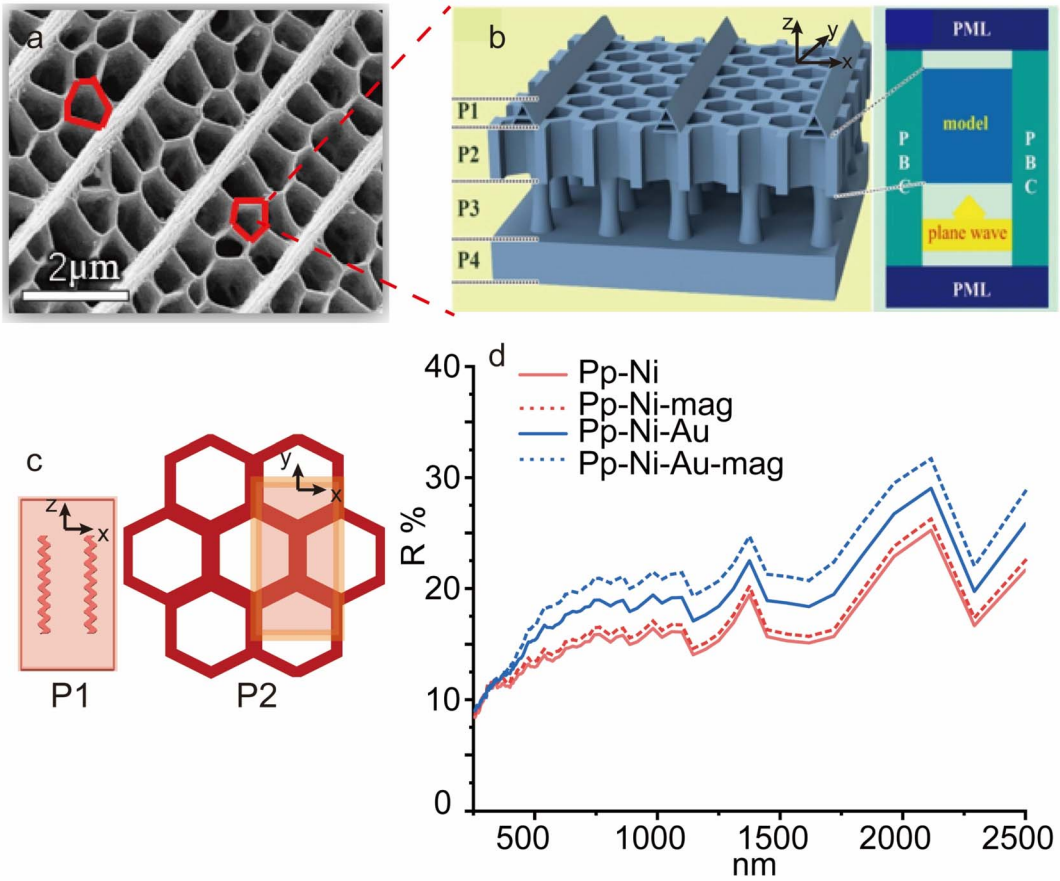


Fig. 5 (a) SEM image of Pp-Ni–Au BWs; (b) theoretical models and boundary conditions of Pp BWs; (c) structural unit applied in Lumerical 2020, *Z* axis denotes the normal of wing scales; (d) simulated reflectance spectra of Pp-Ni and Pp-Ni–Au BWs (250–2500 nm).

## 4. Conclusions

We have used two types of BWs as a template to successfully construct a surface-plasmonic/magneto-optic composite (Ni–Au30 BWs). After chemical coating and self-assembling, the original BWs' hierarchical structures are successfully retained, especially the nature photonic crystal structures of Mm BWs. Through a series of comparative experiments, it is found that only the composite with discrete Au nanoparticles and 3D sub-microstructures exhibits magneto-optical effect. Different from the variation of the angle of polarized light in the magneto-optical Kerr effect[13] or the peak shift in previous studies,[22] the magneto-optical phenomenon we found mainly appears as a change in reflection intensity. Under the magnetic field of 0.3 T, the maximum reflection change in the range of 250–2500 nm is observed on Mm BWs. Mm-Ni BWs' reflectance spectrum increases 3.7% at the reflection peak of 1944 nm, while its Mm-Ni–Au30 BWs counterpart significantly increases 19.6%. The variation amplitude increased 5.3 times because of discrete Au nanoparticles' LSPR. Since our metallic BWs exhibit nearly super-paramagnetic behaviours, this phenomenon might mainly originate from the samples' structural change under external magnetic fields. Given the flexibility and the generality of the templating and the wealth of known and as-yet-undiscovered complex biological structures, they will offer unprecedented model materials to deepen researchers' understanding of the physical principle and coupling process behind MP effect. The further research will provide solid foundation for the future applications of biology sensors, chemical sensors, photonic chips, electrical communication systems and so on.

## Conflicts of interest

There are no conflicts to declare.

## Acknowledgements

The authors acknowledge financial supported from the National Natural Science Foundation of China (No. 52071213, 51971133, 51672175, and 51772187), Science and Technology Commission of Shanghai Municipality (No. 18JC1410500, 16520710900, 17ZR1441400, and 17520710600), and National Key Research and Development Program of China (No. 2017YFE0113000).

## References

1 K. W. Chiu and J. J. Quinn, *Phys. Rev. B: Solid State*, 1972, **5**, 4707.
2 J. J. Brion, R. F. Wallis, A. Hartstein and E. Burstein, *Phys. Rev. Lett.*, 1972, **28**, 1455.

Open Access Article. Published on 11 March 2024. Downloaded on 7/24/2025 9:55:34 AM.
This article is licensed under a Creative Commons Attribution-NonCommercial 3.0 Unported Licence.

3 Y. Li, Q. Zhang, A. V. Nurmikko and S. Sun, *Nano Lett.*, 2005, **5**, 1689.
4 H. Feil and C. Haas, *Phys. Rev. Lett.*, 1987, **58**, 65.
5 S. Jibin, W. Binghui, Z. Zijian, *et al.*, *Angew. Chem., Int. Ed.*, 2017, **129**, 8222.
6 C. Hermann, V. A. Kosobukin, G. Lampel, *et al.*, *Phys. Rev. B: Condens. Matter Mater. Phys.*, 2001, **64**, 235422.
7 A. V. Kimel, A. Kirilyuk, P. A. Usachev, *et al.*, *Nature*, 2005, **435**, 655.
8 P. B. Johnson and R. W. Christy, *Phys. Rev. B: Solid State*, 1972, **6**, 4370.
9 P. B. Johnson and R. W. Christy, *Phys. Rev. B: Solid State*, 1974, **9**, 50561.
10 Y. Li, Q. Zhang, A. V. Nurmikko and S. Sun, *Nano Lett.*, 2005, **5**, 1689.
11 J. Song, B. Wu, Z. Zhou, *et al.*, *Angew. Chem., Int. Ed.*, 2017, **129**, 8222–8226.
12 S. Tomita, T. Kato, S. Tsunashima, *et al.*, *Phys. Rev. Lett.*, 2006, **96**, 167402.
13 F. Dirnberger, J. Quan, R. Bushati, *et al.*, *Nature*, 2023, **620**, 533–537.
14 L. Wu, W. Wang, W. Zhang, *et al.*, *NPG Asia Mater.*, 2018, **10**, e462.
15 Y. W. Tan, J. J. Gu, X. N. Zang, *et al.*, *Angew. Chem., Int. Ed.*, 2011, **50**, 8307–8311.
16 Y. W. Tan, J. J. Gu, L. H. Xu, *et al.*, *Adv. Funct. Mater.*, 2012, **22**, 1578–1585.
17 S. Kinoshita and S. Yoshioka, *ChemPhysChem*, 2005, **6**, 1442–1459.
18 J. A. Garlow, L. K. Barrett, L. Wu, *et al.*, *Sci. Rep.*, 2016, **29**, 19804.
19 T. J. Macdonald, K. Wu, S. K. Sehmi, *et al.*, *Sci. Rep.*, 2016, **16**, 39272.
20 S. Swaminathan, V. G. Rao, J. K. Bera, *et al.*, *Angew. Chem., Int. Ed.*, 2021, **60**, 12532.
21 X. Zhuang, Y. Zhang, C. Cai, *et al.*, *Sci. Rep.*, 2018, **8**, 16379.
22 P. Wenhong, Z. Shenmin, W. Wanlin, *et al.*, *Adv. Funct. Mater.*, 2012, **22**, 2072.


© 2024 The Author(s). Published by the Royal Society of Chemistry